Modeling of Arbitrary Shaped Cables Using Novel Single Source Integral Equation Formulation

A. Menshov, V. Okhmatovski, H.M.J.S.P. De Silva, K.K.M.A. Kariyawasam, J.E. Nordstrom

***Abstract*—This paper proposes a novel method for calculation of frequency dependent parameters for any arbitrary shaped cable based on a new integral equations formulation and its Method of Moment solution. The proposed approach accurately considers both skin and proximity effects. The computation of series impedance matrix using this method is described for a sector-shaped cable example. The frequency domain impedance calculations are compared with alternative techniques such as finite element and sub-conductor methods. Time domain simulation results for open and short circuit terminations are also compared with sub-conductor technique.**

***Keywords*: sector-shaped cables, proximity effect, frequency dependent parameters, method of moment**

I. Introduction

Accurate modeling of cable systems in electro-magnetic transient (EMT) programs is becoming significant with the recent development of underground power transmission systems as a result of environmental policies in many countries.

In power system transient studies, there are increased applications involved in modeling non-conventional cables such as pipe type cables, sector-shaped cables, umbilical cables etc. Compared with traditional coaxial cables, the electro-magnetic transient (EMT) modelling of such non-conventional cables is challenging. The accurate consideration of proximity effect as well as skin effect is required to calculate frequency dependent parameters for such configurations.

This paper proposes a general approach for electromagnetic transient modelling of any arbitrary shaped multi-conductor cable. Frequency dependent resistances and inductances of the cable are obtained using a Method of Moment (MoM) discretization of a novel single source integral equation [1]-[2].

The EMT modeling of pipe type cable based on MoM method is described in [3]. In this paper, the impedance operator is analytically derived for circular domains; hence cables or cable bundles in which each cable is of circular shape can be only handled. For every other cross-section shape, a new surface impedance operator has to be created. However the proposed method is truly general in terms of the cross-sectional shapes while featuring the same number of MoM unknowns as [3].

Alternatively, sub-conductor technique [4], [6] or finite element method [8] can be used to find parameters for non-conventional cables. However above methods require significantly higher computational time and effort. For 100 frequency samples, corresponding Z and Y matrices can be generated within minutes using proposed method. The sub-conductor technique requires approximately half an hour and the finite element method (FEM) requires more than an hour.

The application of this technique is demonstrated using a sector shaped cable example. The series impedance (Z) matrices are compared with an alternative sub-conductor technique proposed in [4] and also with the FEM approach [8].

The frequency domain characteristics are discussed and propagation modes are analyzed by plotting velocities and attenuation of the modes as a function of frequency. The time domain results for step voltage excitation with linear impedance terminations are compared for the proposed method and the sub-conductor technique.

II. Surface-Volume-Surface Electric Field Integral Equation Formulation

Consider a power cable consisting of N_c conductors of arbitrary cross-section. We denote the index identifying the conductor number as $\alpha = 1, \ldots, N_c$. The contour bounding the cross-section of the α th conductor and the cross-section itself are indicated as ∂S_α and S_α, respectively. Under the quasi-static approximation, we can write the traditional Volume Electric Field Integral Equation (V-EFIE) in terms of the volumetric current density j

$$\frac{j(\boldsymbol{\rho})}{\sigma} + i\omega\mu_0 \iint_S ds' G_0(\boldsymbol{\rho},\boldsymbol{\rho}')\, j(\boldsymbol{\rho}') = -V_{\text{p.u.l.}}, \boldsymbol{\rho} \in S, \quad (1)$$

where $G_0(\boldsymbol{\rho},\boldsymbol{\rho}') = -\frac{1}{2\pi}\ln|\boldsymbol{\rho}-\boldsymbol{\rho}'|$ is the quasi-static Green's function of free-space, σ is the conductor bulk conductivity, μ_0 is the permeability of free space, ω is the cyclic

A. Menshov is with the Dept. of Electrical and Computer Eng., University of Texas, United States (e-mail of corresponding author: anton.menshov@gmail.com)
V. Okhmatovski is with the Dept. of Electrical and Computer Eng., University of Manitoba, Canada
(e-mail: Vladimir.Okhmatovski@umanitoba.ca)
H.M.J.S.P. De Silva, K. K. M. A. Kariyawasam and J.E. Nordstrom are with the Manitoba HVDC Research Centre, Canada (email: jeewantha@hvdc.ca, akariyawasam@hvdc.ca, johnn@pscad.com).

Paper submitted to the International Conference on Power Systems Transients (IPST2015) in Cavtat, Croatia June 15-18, 2015

frequency, i is the imaginary unit, $\boldsymbol{\rho}$ and $\boldsymbol{\rho}'$ are position vectors to the observation and source points, respectively, and $V_{\text{p.u.l.}}$ is the per unit length voltage drop along the conductor cross-section.

If the conductivity σ is homogeneous for each of the conductors constituting the cable, the electric field inside the conductor satisfies the homogeneous Helmholtz equation. In [1], [2], this fact is taken into account in order to derive a novel single source Surface-Volume-Surface Electric Field Integral Equation (SVS-EFIE) in terms of the unknown surface current density J defined on the contours ∂S_α bounding conductor's cross-sections

$$\begin{aligned} &-i\omega\mu_0 \oint_{\partial S_\alpha} dc' G_\sigma^\alpha(\boldsymbol{\rho},\boldsymbol{\rho}')\, J_\alpha(\boldsymbol{\rho}') - (\omega\mu_0)^2 \\ &\sum_{\alpha'=1}^{N_c} \sigma_{\alpha'} \iint_{S_{\alpha'}} ds' G_0(\boldsymbol{\rho},\boldsymbol{\rho}') \oint_{\partial S_{\alpha'}} dc'' G_\sigma^{\alpha'}(\boldsymbol{\rho}',\boldsymbol{\rho}'')\, J_{\alpha'}(\boldsymbol{\rho}'') \\ &= -V_{\text{p.u.l.}}, \boldsymbol{\rho} \in \partial S_\alpha,\ \alpha = 1,\ldots,N_c \end{aligned} \tag{2}$$

where $G_\sigma^\alpha(\boldsymbol{\rho},\boldsymbol{\rho}')$ is Green's function of the αth conductor medium

$$\begin{aligned} G_\sigma^\alpha(\boldsymbol{\rho},\boldsymbol{\rho}') &= -\frac{i}{4} H_0^{(2)}\left(k_\sigma^\alpha \left|\boldsymbol{\rho}-\boldsymbol{\rho}'\right|\right), \\ k_\sigma^\alpha(\omega,\sigma) &= \sqrt{-i\omega\mu_0\sigma_\alpha}. \end{aligned} \tag{3}$$

In (3), $H_0^{(2)}$ is the second-kind Hankel function of zeroth order, and k_σ^α is the wavenumber of αth conductor.

The SVS-EFIE (2) can be conveniently written in the following operator form

$$\mathcal{T}_{\sigma_{\alpha'}}^{\partial S,\partial S} \circ J_\alpha + \sum_{\alpha'=1}^{N_c} \sigma_{\alpha'} \mathcal{T}_0^{\partial S,S} \circ \mathcal{T}_{\sigma_{\alpha'}}^{S,\partial S} \circ J_{\alpha'} = -V_{\text{p.u.l.}}. \tag{4}$$

The operators entering (4) are defined, as follows:

$$\mathcal{T}_{\sigma_{\alpha'}}^{\partial S,\partial S} \circ J_\alpha = -i\omega\mu_0 \oint_{\partial S_\alpha} dc' G_\sigma^\alpha(\boldsymbol{\rho},\boldsymbol{\rho}')\, J_\alpha(\boldsymbol{\rho}'),\ \boldsymbol{\rho} \in \partial S_\alpha, \tag{5}$$

$$\mathcal{T}_0^{\partial S,S} \circ j_{\alpha'} = -i\omega\mu_0 \iint_{S_{\alpha'}} ds' G_0(\boldsymbol{\rho},\boldsymbol{\rho}') j_{\alpha'}(\boldsymbol{\rho}'),\ \boldsymbol{\rho} \in \partial S_\alpha, \tag{6}$$

$$\mathcal{T}_{\sigma_{\alpha'}}^{S,\partial S} \circ J_{\alpha'} = -i\omega\mu_0 \oint_{\partial S_{\alpha'}} dc' G_\sigma^{\alpha'}(\boldsymbol{\rho},\boldsymbol{\rho}') J_{\alpha'}(\boldsymbol{\rho}'),\ \boldsymbol{\rho} \in S_{\alpha'}. \tag{7}$$

The SVS-EFIE (2) involves the integral operators that map the unknown surface current density from the conductor boundary ∂S_α to the conductor cross-section S_α and back to the boundary for each αth conductor. Therefore, the Method of Moments (MoM) discretization of the SVS-EFIE requires both contour and surface meshes. Each conductor boundary ∂S_α is discretized with M_α linear elements, and cross-section S_a – with N_α triangles. A detailed description of the MoM discretization of the SVS-EFIE (2) is given in our previous publications for a two-conductor [2] and co-axial cable [1] cases.

After each of the integral operators is discretized, the SVS-EFIE (2) is reduced to a set of $M = M_1 + M_2 + \ldots + M_{N_c}$ linear algebraic equations with M unknowns

$$\left(\mathbf{Z}_\sigma^{\partial S,\partial S} + \mathbf{Z}_0^{\partial S,S} \cdot \mathbf{Z}_\sigma^{S,\partial S}\right) \cdot \mathbf{I} = \mathbf{V}, \tag{8}$$

where $\mathbf{Z}_\sigma^{\partial S,\partial S}, \mathbf{Z}_0^{\partial S,S}$ and $\mathbf{Z}_\sigma^{S,\partial S}$ are the discretized versions of the SVS-EFIE contour-to-contour (5), surface-to-contour (6), and contour-to-surface (7) operators in a block form, respectively [2]. We will depict the overall matrix structure of the SVS-EFIE (8) for the example of a sectorial cable with an outer conductor ($\alpha = 1$) and three inner conductors ($\alpha = 2, 3, 4$).The outer conductor $\alpha = 1$ has two contours ∂S_{1a} and ∂S_{1b} forming its "shell" cross-section.

The discretized versions of the contour-to-contour operator $\mathbf{Z}_\sigma^{\partial S,\partial S}$, surface-to-contour operator $\mathbf{Z}_0^{\partial S,S}$, and contour-to-surface operator $\mathbf{Z}_\sigma^{S,\partial S}$ are the matrices of the following form

$$\mathbf{Z}_\sigma^{\partial S,\partial S} = \overbrace{\begin{bmatrix} \left[\mathbf{Z}_\sigma^{\partial S_{1a},\partial S_{1a}}\right] & \left[\mathbf{Z}_\sigma^{\partial S_{1a},\partial S_{1b}}\right] & \mathbf{0} & \mathbf{0} & \mathbf{0} \\ \left[\mathbf{Z}_\sigma^{\partial S_{1b},\partial S_{1a}}\right] & \left[\mathbf{Z}_\sigma^{\partial S_{1b},\partial S_{1b}}\right] & \mathbf{0} & \mathbf{0} & \mathbf{0} \\ \mathbf{0} & \mathbf{0} & \left[\mathbf{Z}_\sigma^{\partial S_2,\partial S_2}\right] & \mathbf{0} & \mathbf{0} \\ \mathbf{0} & \mathbf{0} & \mathbf{0} & \left[\mathbf{Z}_\sigma^{\partial S_3,\partial S_3}\right] & \mathbf{0} \\ \mathbf{0} & \mathbf{0} & \mathbf{0} & \mathbf{0} & \left[\mathbf{Z}_\sigma^{\partial S_4,\partial S_4}\right] \end{bmatrix}}^{M\times M}, \tag{9}$$

$$\mathbf{Z}_0^{\partial S,S} = \overbrace{\begin{bmatrix} \left[\mathbf{Z}_0^{\partial S_{1a},S_1}\right] & \left[\mathbf{Z}_0^{\partial S_{1a},S_2}\right] & \left[\mathbf{Z}_0^{\partial S_{1a},S_3}\right] & \left[\mathbf{Z}_0^{\partial S_{1a},S_4}\right] \\ \left[\mathbf{Z}_0^{\partial S_{1b},S_1}\right] & \left[\mathbf{Z}_0^{\partial S_{1b},S_2}\right] & \left[\mathbf{Z}_0^{\partial S_{1b},S_3}\right] & \left[\mathbf{Z}_0^{\partial S_{1b},S_4}\right] \\ \left[\mathbf{Z}_0^{\partial S_2,S_1}\right] & \left[\mathbf{Z}_0^{\partial S_2,S_2}\right] & \left[\mathbf{Z}_0^{\partial S_2,S_3}\right] & \left[\mathbf{Z}_0^{\partial S_2,S_4}\right] \\ \left[\mathbf{Z}_0^{\partial S_3,S_1}\right] & \left[\mathbf{Z}_0^{\partial S_3,S_2}\right] & \left[\mathbf{Z}_0^{\partial S_3,S_3}\right] & \left[\mathbf{Z}_0^{\partial S_3,S_4}\right] \\ \left[\mathbf{Z}_0^{\partial S_4,S_1}\right] & \left[\mathbf{Z}_0^{\partial S_4,S_2}\right] & \left[\mathbf{Z}_0^{\partial S_4,S_3}\right] & \left[\mathbf{Z}_0^{\partial S_4,S_4}\right] \end{bmatrix}}^{M\times N}, \tag{10}$$

$$\mathbf{Z}_\sigma^{S,\partial S} = \overbrace{\begin{bmatrix} \left[\mathbf{Z}_\sigma^{S_1,\partial S_{1a}}\right] & \left[\mathbf{Z}_\sigma^{S_1,\partial S_{1b}}\right] & \mathbf{0} & \mathbf{0} & \mathbf{0} \\ \mathbf{0} & \mathbf{0} & \left[\mathbf{Z}_\sigma^{S_2,\partial S_2}\right] & \mathbf{0} & \mathbf{0} \\ \mathbf{0} & \mathbf{0} & \mathbf{0} & \left[\mathbf{Z}_\sigma^{S_3,\partial S_3}\right] & \mathbf{0} \\ \mathbf{0} & \mathbf{0} & \mathbf{0} & \mathbf{0} & \left[\mathbf{Z}_\sigma^{S_4,\partial S_4}\right] \end{bmatrix}}^{N\times M}. \tag{11}$$

The structure of the matrices is determined by the nature of the integral operator of the SVS-EFIE (2). The discretized version of contour-to-contour operator $\mathbf{Z}_\sigma^{\partial S,\partial S}$ (9) and contour-to-surface operator $\mathbf{Z}_{\sigma}^{S,\partial S}$ (11) correspond to the interactions inside a given conductor via full-wave Green's function of the conductor medium (3). Therefore, only block-diagonal entries are present. Moreover, as frequency of the analysis grows, so does the sparsity of the block-entries in (9) and (11) due to exponential attenuation of the Green's function (3). As the cross-sectional current becomes negligible beyond a few skin-depths, some of the entries in (9), (10), and (11) can be preemptively zeroed out based on the tolerance β. It implies that all elements in the matrices $\mathbf{Z}_{\sigma}^{\partial S,\partial S}$ (9) and $\mathbf{Z}_{\sigma}^{S,\partial S}$ (11) representing the interactions between the elements that are separated by a distance larger than L will not be calculated and stored.

$$L = \beta\delta(f,\sigma) = \beta\,\mathrm{Re}(k_{\sigma}(f,\sigma)) = \beta\sqrt{\frac{1}{\pi f \mu_0 \sigma}} \qquad (12)$$

It is worth to note, that some entries in $\mathbf{Z}_{0}^{\partial S,S}$ (10) can be zeroed out as well based on the structure of the matrix $\mathbf{Z}_{\sigma}^{S,\partial S}$ (11) after applying the skin-depth based tolerance criteria (12).

The matrix form of the SVS-EFIE (8) is solved numerically for M unknown coefficients $\mathbf{I}$ in the expansion of the surface current density on the conductor's cross-section boundaries ∂S. Then, N samples of the volumetric current density $\mathbf{j}$ in the cable cross-section S can be obtained using the discretized contour-to-surface operator $\mathbf{Z}_{\sigma}^{S,\partial S}$ (11) maps the auxiliary surface current density to the volumetric current in the cross-section of the conductor, as follows

$$\mathbf{j} = \mathbf{Z}_{\sigma}^{S,\partial S} \cdot \mathbf{I}. \qquad (13)$$

The expressions for the actual matrix entries can be found in [2] for the discretization with pulse basis functions both on the conductor boundary ∂S and conductor cross-section S.

III. Inclusion of Ground and Formulation of the Admittance Matrix

The Z matrix formulated as discussed in section II represents the impedance due to skin and proximity effects of all the conductors in the sector-shaped cable. The impedance of the insulation and the ground are added to obtain full Z matrix as discussed in [4], [5]. The ground impedance is evaluated using the closed form approximate formula [7].

The formulation of admittance matrix is described in reference [4] and hence not discussed here.

IV. Example Case Study

An example case involving a sector-shaped cable is used to demonstrate the proposed method. The cable configuration and data [4] are shown in Fig 1 and Table 1 respectively.

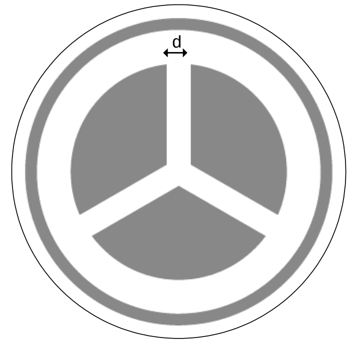

Fig 1: Sector-shaped cable example

TABLE I
Cable Data

Inner conductor radius	19 mm
Sheath inner radius	25 mm
Sheath outer radius	27 mm
Cable outer radius	30 mm
Inter-conductor distance, d	4.255 mm
Inter-conductor conductivity	58000 S/mm
Sheath conductivity	1100 S/mm
Relative permittivity of inner insulation	4.1
Relative permittivity of outer insulation	2.3

The comparison of self and mutual impedances is shown in tables from I to IV. The finite element method and sub-conductor results are obtained from [4], [8]. The impedance calculation using proposed MOM method is in a close agreement with the FEM approach and also with sub-conductor technique.

TABLE I
SELF RESISTANCE COMPARISON

Frequency (Hz)	Resistance (Ω/km)			Difference (MOM and FEM) (%)
	Finite Element method	Sub-conductor Method	Proposed MOM-method	
6	2.8400	2.8400	2.8420	0.0704
60	2.8499	2.8499	2.8516	0.0597
600	2.9675	2.9608	2.9672	0.0101
6E+03	3.5250	3.5076	3.4979	0.7688
60E+03	5.1505	5.2022	4.9690	3.5239

TABLE II
MUTUAL RESISTANCE COMPARISON

Frequency (Hz)	Resistance (Ω/km)			Difference (MOM and FEM) (%)
	Finite Element method	Sub-conductor Method	Proposed MOM-method	
6	2.7825	2.7824	2.7843	0.0647
60	2.7832	2.7833	2.7850	0.0647
600	2.7804	2.7871	2.7847	0.1547
6E+03	2.6946	2.7090	2.6941	0.0186
60E+03	2.8882	2.7693	2.8299	2.0186

TABLE III
SELF INDUCTANCE COMPARISON

Frequency (Hz)	Inductance (μH/km)			Difference (%) (MOM and FEM)
	Finite Element method	Sub-conductor Method	Proposed MOM-method	
6	232.02	229.98	232.2283	0.0898
60	220.67	218.32	221.0065	0.1525
600	156.80	155.35	157.0402	0.1532
6E+03	120.40	121.61	120.7107	0.2581
60E+03	105.09	107.42	105.6883	0.5693

TABLE IV
MUTUAL INDUCTANCE COMPARISON

Frequency (Hz)	Inductance (μH/km)			Difference (%) (MOM and FEM)
	Finite Element method	Sub-conductor Method	Proposed MOM-method	
6	40.445	40.833	40.3621	0.2050
60	40.191	40.207	40.1380	0.1319
600	35.722	34.627	35.7320	0.0280
6E+03	38.324	35.607	38.3511	0.0707
60E+03	40.692	37.524	40.8166	0.3062

The propagation constants γ of the natural modes are defined as eigenvalues of $\sqrt{ZY}$ matrix [5]. The attenuation coefficient α and the modal velocity v are defined as,

$$\alpha = \mathrm{Re}\{\gamma\} \tag{9}$$

$$v = \omega / Im\{\gamma\} \tag{10}$$

Where, $\omega = 2\pi f$, f is the frequency in Hz. Fig. 2 and 3 show the attenuation coefficient and the velocity characteristics of all modes. It can be seen that mode 1 is a zero sequence mode with relatively high attenuation and low velocity. Mode 2 is a sheath to conductor mode and modes 3 and 4 are inter-conductor modes.

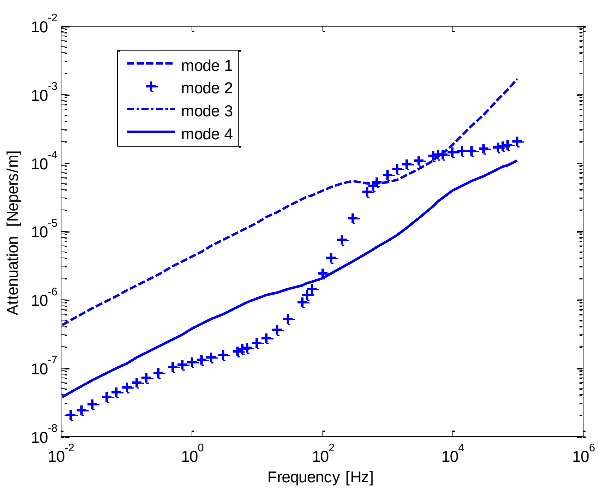

Fig 2: Frequency dependence of attenuation constant α

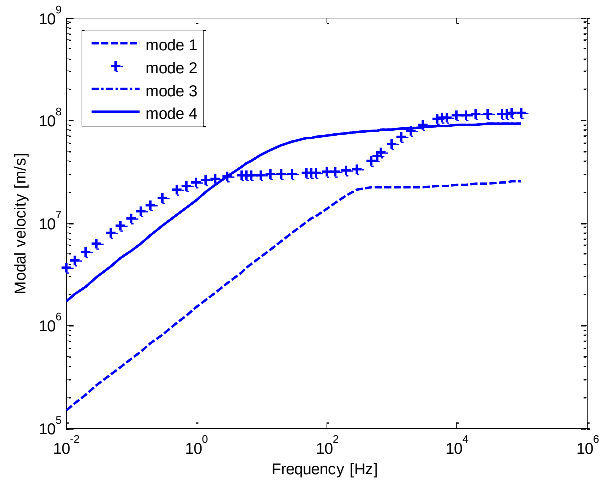

Fig 3: Frequency dependence of modal velocity v

The propagation and characteristic admittance matrices are calculated as described in [5]. The length of the cable is assumed to be 20 km. Fig 4 and 5 show the comparison of first column of the propagation matrix and the characteristic admittance matrix calculated using MOM method (solid lines) and the sub-conductor technique ('+' sign). The proposed MOM method is in a good agreement with sub-conductor method.

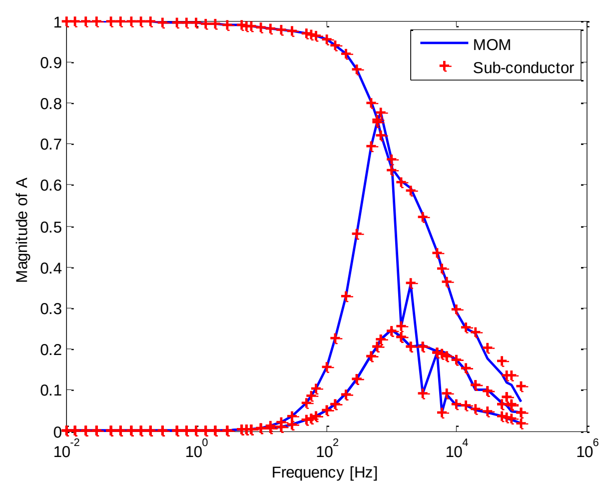

Fig 3: First column of the propagation matrix

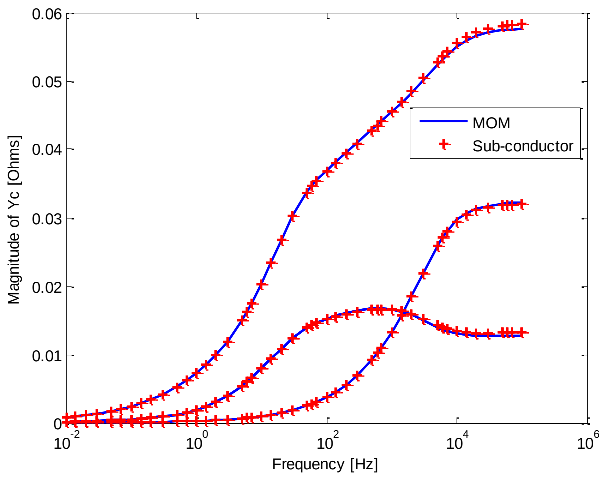

Fig 4: First column of characteristic admittance matrix

V. Time domain simulation results

Time domain simulations for open circuit and short circuit terminations are performed using PSCAD/EMTDC commercial software as shown in Fig. 5. The calculated Z and Y matrices are added to the transmission line model (Universal Line model [9]) through external file using the multiple-frequency external input option. The cable is energized with a 1 kV step voltage.

Fig. 6 shows the induced voltage in the third conductor for open circuit termination for time period up to 0.01 sec. The simulation results from proposed method (solid lines) are compared with that of sub-conductor method (dashed line).The two methods are in a close agreement. Fig. 7 shows the sending-end current from the same excitation for short circuit terminations. Again the two waveforms are in a close agreement verifying the accuracy of the proposed MOM method. Note that the results from sub-conductor technique have been already verified with Numerical Inverse Lapalce Solution in [4].

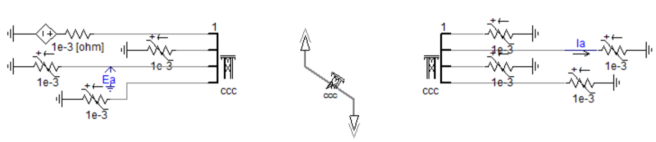

Fig 5: Excitation and termination configurations in the time domain simulation.

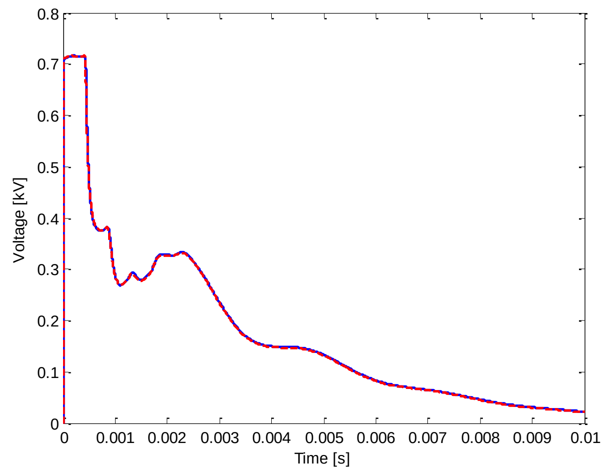

Fig 6: Transient behavior of the induced voltage

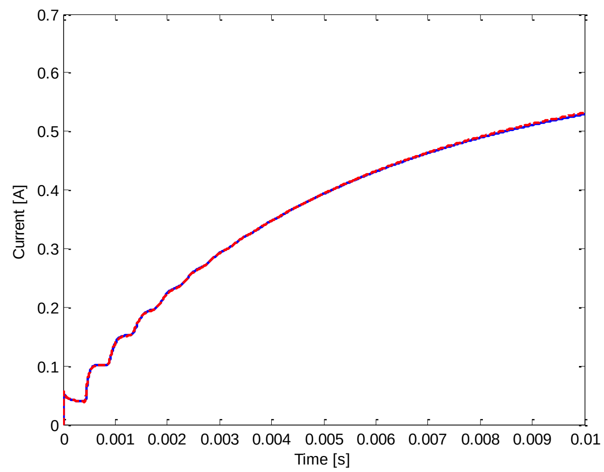

Fig 7: Transient behavior of the sending-end current

VI. Conclusion

The proposed MOM based method can be used to accurately simulate non-conventional cable configurations such as sector-shaped cables. The frequency domain parameters from the proposed method are in a good agreement with alternative techniques such as the sub-conductor method and also finite element method. Also the time domain simulation results are in a close agreement with the proposed method. The main advantage of the method is that the computational time is significantly less compared with the above alternative techniques. Compared to the similar method discussed in [3], the proposed method is truly general in terms of the cross-sectional shapes.

VII. References

[1] A. Menshov and V. Okhmatovski, “Method of moment solution of Surface-Volume-Surface Electric Field Integral Equation for two-dimensional transmission lines of complex cross-sections,” in 2012

IEEE 16th Workshop on Signal and Power Integrity (SPI), 2012, pp. 31–34.

[2] A. Menshov and V. Okhmatovski, "New Single-Source Surface Integral Equations for Scattering on Penetrable Cylinders and Current Flow Modeling in 2-D Conductors," IEEE Trans. Microw. Theory Tech., vol. 61, no. 1, pp. 341–350, Jan. 2013.

[3] U. R. Patel, B. Gustavsen, and P. Triverio, "Application of the MoM-SO Method for Accurate Impedance Calculation of Single-Core Cables Enclosed by a Conducting Pipe ", IPST 2013, July 2013.

[4] K.K.M.A. Kariyawasam, A. M. Gole, B. Kordi, H.M.J.S.P. De Silva, "Accurate Electromagnetic Transient Modelling of Sector-Shaped Cables", IPST 2011, June 2011.

[5] L. M. Wedepohl, D. J. Wilcox, "Transient Analysis of Underground Power-Transmission Systems - System Modal and Wave-Propagation Characteristics", Proc. IEE, Vol. 120, No. 2, Feb. 1973, p. 253 - 260. (8 pages)

[6] P. de Arizón and H. W. Dommel, "Computation of cable impedances based on subdivision of conductors", *IEEE Transactions on Power Delivery,* vol. 2, pp. 21–27, Jan. 1987.

[7] O. Saad, G. Gaba, M. Giroux, "A Closed-Form Approximation for Ground Return Impedence of Underground Cables", *IEEE Transactions on Power Delivery,* vol. 11, pp. 1536–1545, Jul. 1996.

[8] R. Rivas, "Calculation of Frequency-Dependant Parameters of Power Cables with Digital Imaging and Partial Subconductors", Ph.D. dissertation, Dept. of Elect. & Comp. Eng., Univ. British Columbia, July 2001.

[9] A. Morched, B. Gustavsen, M. Tartibi, "A universal model for accurate calculation of electromagnetic transients on overhead lines and underground cables", *IEEE Transactions on Power Delivery*, vol.14, no.3, pp.1032-1038, Jul 1999.